

Dependence of magnetic susceptibility on stress in textured polycrystalline $\text{Fe}_{81.6}\text{Ga}_{18.4}$ and $\text{Fe}_{79.1}\text{Ga}_{20.9}$ Galfenol alloys

A. Mahadevan, P. G. Evans, and M. J. Dapino^{a)}

Department of Mechanical Engineering, The Ohio State University, Columbus, Ohio 43210, USA

(Received 18 November 2009; accepted 9 December 2009; published online 5 January 2010)

Magnetization and magnetostriction measurements in constant tension and compression as a function of applied magnetic field are reported for $\langle 100 \rangle$ oriented, textured polycrystalline $\text{Fe}_{81.6}\text{Ga}_{18.4}$ and $\text{Fe}_{79.1}\text{Ga}_{20.9}$ Galfenol alloys. The susceptibility change with stress, or sensitivity, is maximum at zero field for both alloys. The greatest sensitivity is observed for the 18.4 at. % Ga alloy between -10 and $+20$ MPa, where domain wall motion dominates. The sensitivity is greater for the 20.9 at. % Ga alloy than for the 18.4 at. % Ga alloy below -15 MPa (domain rotation region). The difference in behavior is attributed to a difference in the anisotropy coefficient.

© 2010 American Institute of Physics. [doi:10.1063/1.3280374]

Magnetostrictive materials provide a robust mechanism for bidirectional conversion of energy between the magnetic and elastic states.¹ Magnetostrictive iron–gallium alloys (Galfenol) are particularly promising as they exhibit high magnetostriction and steel-like mechanical properties,² enabling transducers for harsh environments.³ The magnetostriction constants and other properties of Galfenol have been shown to depend heavily on Ga content.⁴ It is therefore necessary to identify optimal ranges of Ga content for transducer applications. It was shown that the domain rotation region of the magnetization is promising for force sensing.⁵ A model for the dependence of susceptibility on stress σ was developed for the domain rotation magnetization process,

$$\chi(\sigma) = \frac{\mu_0 M_s^2}{2K_4 - 3\lambda_{100}\sigma}. \quad (1)$$

The reported measurements of $\text{Fe}_{81.5}\text{Ga}_{18.5}$ and $\text{Fe}_{79.1}\text{Ga}_{20.9}$ along with Eq. (1) suggest that 19–22 at. % Ga is a good range for force sensors based on domain rotation, because of a very low anisotropy constant K_4 and still moderate saturation magnetization M_s and magnetostriction λ_{100} .

The reported magnetization measurements of $\text{Fe}_{79.1}\text{Ga}_{20.9}$ are for single-crystalline material in compression only. In this work, measurements of textured polycrystalline $\text{Fe}_{79.1}\text{Ga}_{20.9}$ and $\text{Fe}_{81.6}\text{Ga}_{18.4}$ from Etrema Products Inc. are performed. This grade is advantageous for its reduced cost of production. The measurements are of magnetization and magnetostriction from applied field at constant stress, including for tensile stress. Motivated by actuation applications, the saturation magnetostriction in the tensile region has been reported previously⁶ but the susceptibility of Galfenol, important for sensing, has not been measured in tension. The measurements in this work indicate that with regard to sensitivity, $\text{Fe}_{81.6}\text{Ga}_{18.4}$ is better for force sensors utilizing the domain wall motion magnetization process and $\text{Fe}_{79.1}\text{Ga}_{20.9}$ is better for force sensors utilizing the domain rotation magnetization process. While the susceptibility during the domain wall motion process has a region with high sensitivity to stress, this region is limited. The stress-dependent suscep-

tibility for the domain rotation process follows the simple inverse relationship in Eq. (1) which has an infinite range of applicability, from negative infinity to the stress value marking the onset of domain wall motion.

The magnetic flux density and magnetostriction of research grade $\langle 100 \rangle$ oriented, textured polycrystalline Galfenol of 18.4 at. % Ga (sample 1) and 20.9 at. % Ga (sample 2) were measured under applied magnetic field at constant stress. An MTS 831.1 elastomer test frame with hydraulic grips was used to apply a constant bias stress from -56.63 to 56.63 MPa prior to magnetic field application. A sinusoidal magnetic field at 0.1 Hz was applied using a closed magnetic circuit with a flux return path. The flux density was measured using a Walker Scientific MF 5D fluxmeter and a pick-up coil midway along the length of the Galfenol rod. The magnetic field was measured at the surface of the rod midway along its length using a Walker Scientific MG-4D Gaussmeter. The magnetization is calculated by subtracting the applied field from the flux density measurement. The differential susceptibility is calculated by the ratio of the change in magnetization to the change in the applied field.

The magnetization curves for sample 1 at constant stress are shown in Fig. 1. They show a steep rise in magnetization

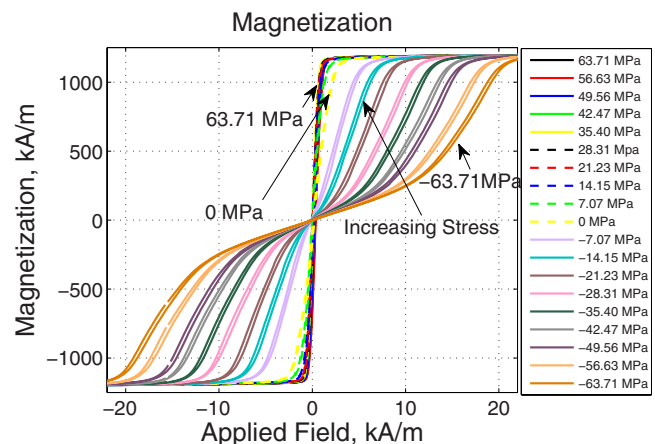


FIG. 1. (Color online) Magnetization curves for $\text{Fe}_{81.6}\text{Ga}_{18.4}$ at constant stress. All measurements presented here were conducted at stresses of 63.71, 56.63, 49.56, 42.47, 35.4, 28.31, 21.23, 14.15, 7.07, 0, -7.07 , -14.15 , -21.23 , -28.31 , -35.4 , -42.47 , -49.56 , -56.63 , and -63.71 MPa.

^{a)} Author to whom correspondence should be addressed. Electronic mail: dapino.1@osu.edu.

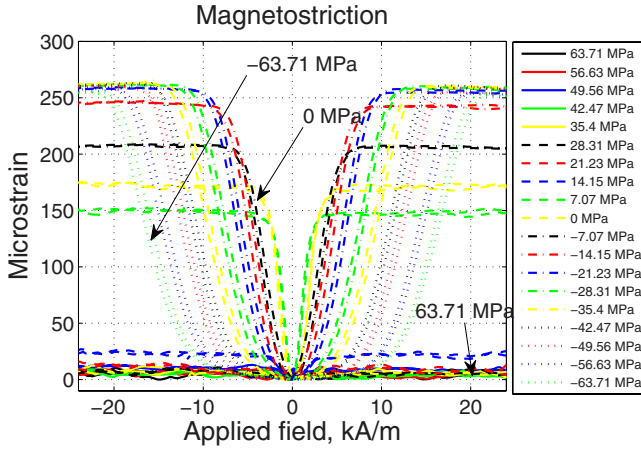


FIG. 2. (Color online) Magnetostriction curves for $\text{Fe}_{81.6}\text{Ga}_{18.4}$ at constant stress.

at zero applied field under tensile stress and a distinct kinking behavior under compressive stress. The magnetostriction curves are shown in Fig. 2. The saturation magnetostriction λ_{sat} decreases with increasing tensile stress and drops to zero at 21.23 MPa and higher tension. With increasing compressive stress up to -49.56 MPa, λ_{sat} increases; there is a slight drop in λ_{sat} at -56.63 and -63.71 MPa. This phenomenon has been previously observed.⁷ From the measurements at saturation, $M_s = 1200$ kA/m and $(3/2)\lambda_{100} = 265 \times 10^{-6}$ (from the -49.5 MPa measurement.) The anisotropy constant is calculated from Eq. (1), $K_4 = 20$ kJ/m³.

The magnetization curves for sample 2 at constant stress are shown in Fig. 3. The behavior of sample 2 is similar to sample 1 under tension, but under compression the kinking observed in sample 1 is less evident. The magnetostriction curves at constant stress are shown in Fig. 4. With increasing tensile stress, λ_{sat} approaches zero and is negligible at 35.4 MPa and higher tension. With increasing compressive stress up to -49.56 MPa, λ_{sat} increases. Again there is a slight drop in λ_{sat} , occurring at -56.63 and -63.71 MPa. From the measurements at saturation, $M_s = 1160$ kA/m and $(3/2)\lambda_{100} = 200 \times 10^{-6}$ (from the -49.56 MPa measurement.) The anisotropy constant is calculated from Eq. (1), $K_4 = 1$ kJ/m³. The saturation magnetostriction is in general less for sample 2 compared to sample 1. In the case of sample 2, the anisotropy coefficient is low, which agrees with reported measure-

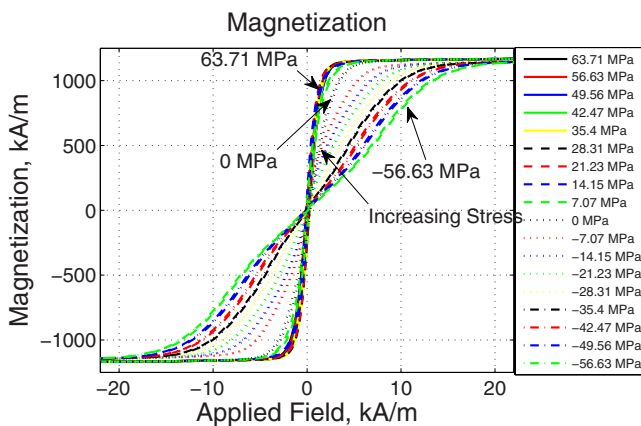


FIG. 3. (Color online) Magnetization curves for $\text{Fe}_{79.1}\text{Ga}_{20.9}$ at constant stress.

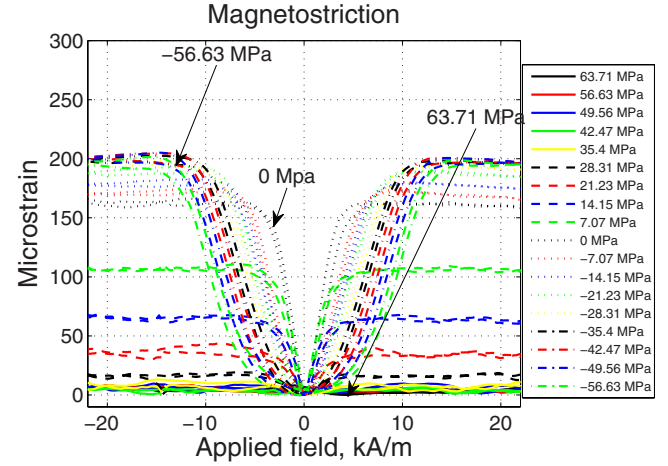


FIG. 4. (Color online) Magnetostriction curves for $\text{Fe}_{79.1}\text{Ga}_{20.9}$ at constant stress.

ments for single crystals.⁸ Hence, domain rotation is dominated by stress anisotropy rather than magnetocrystalline anisotropy at all applied fields until saturation.

The differential susceptibility is calculated from the magnetization measurements. Figure 5 shows the susceptibility of sample 1 as a function of magnetic field at constant stress. A single peak occurs at zero field when no stress is applied and for tensile stress. The kinking behavior observed in the magnetization measurements manifests as two peaks, symmetric about zero field; the valley at low applied fields is due to stress-dependent domain rotation. The higher magnetocrystalline anisotropy of sample 1 is responsible for the kinking behavior shown in the magnetization curves where the steep regions of magnetization are from rapid growth of domains parallel to the field at the expense of domains oriented perpendicular to it; this occurs through domain wall motion.⁹

Figure 6 shows the susceptibility of sample 2 as a function of magnetic field at constant stress. The susceptibility curves with tensile stress are similar to those of sample 1, but the magnitude of the peak susceptibility at zero applied field for the same stress is much lower. The peaks are less sharp compared to the susceptibility curves of sample 1. The

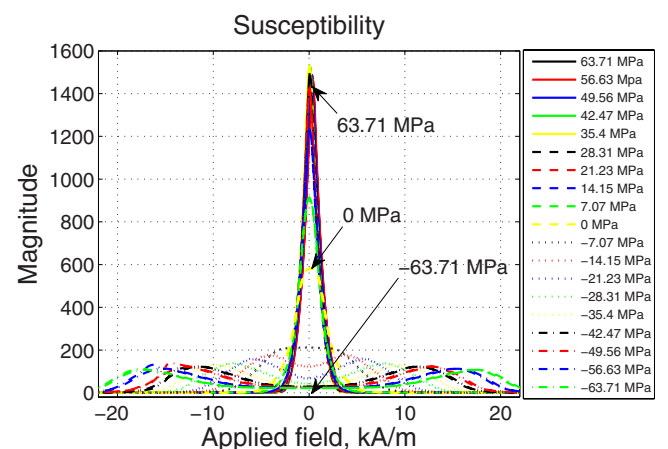


FIG. 5. (Color online) Susceptibility at constant stress for $\text{Fe}_{81.6}\text{Ga}_{18.4}$.

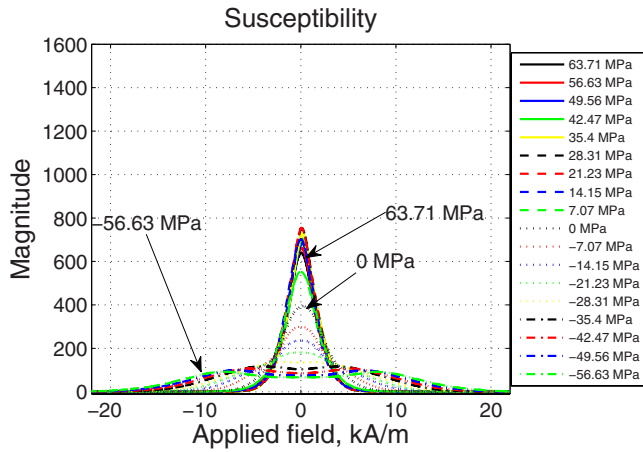


FIG. 6. (Color online) Susceptibility at constant stress for $\text{Fe}_{79.1}\text{Ga}_{20.9}$.

difference is due to the low crystal anisotropy of sample 2 in relation to the saturation magnetization and magnetostriction.

The susceptibility change as a function of stress is maximum at zero applied field for both samples. This is plotted in Fig. 7. Sample 1 has a larger magnitude of susceptibility at all tensile stresses. The susceptibility change of sample 1 is greatest at stresses ranging from -10 to $+20$ MPa, where domain wall motion is the dominant process. Sample 2 has a greater susceptibility and sensitivity to stress in the compressive region below -10 MPa where domain rotation is the dominant process. The former is advantageous in terms of linearity and the latter is advantageous in terms of stress range. These measurements can be used to design a force or torque sensor working on the principle of stress dependent susceptibility.

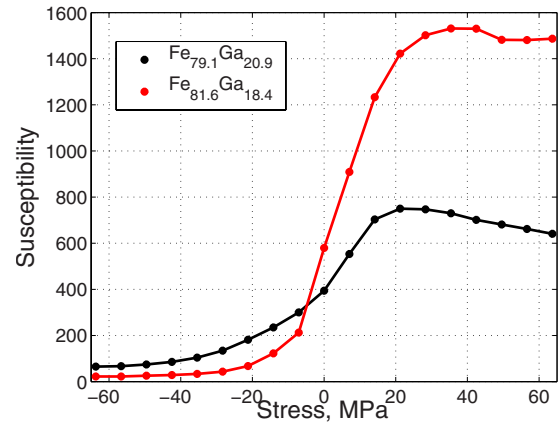


FIG. 7. (Color online) Stress dependent susceptibility at zero applied field.

We wish to acknowledge the financial support by the Office of Naval Research, MURI Grant No. N000140610530, and by Moog Inc.

¹M. J. Dapino, *Struct. Eng. Mech.* **17**, 303 (2004).

²A. E. Clark, J. B. Restorff, M. Wun-Fogle, T. A. Lograsso, and D. L. Schlagel, *IEEE Trans. Magn.* **36**, 3238 (2000).

³R. Myers, R. A. Islam, M. Karmarkar, and S. Priya, *Appl. Phys. Lett.* **91**, 122904 (2007).

⁴M. Wuttig, L. Dai, and J. Cullen, *Appl. Phys. Lett.* **80**, 1135 (2002).

⁵M. Wun-Fogle, H. T. Savage, and A. E. Clark, *Sensors and Actuators* **12**, 323 (1987).

⁶M. Wun-Fogle, J. B. Restorff, and A. E. Clark, *J. Intell. Mater. Syst. Struct.* **17**, 117 (2006).

⁷J. Atulasimha, A. B. Flatau, and J. R. Cullen, *Smart Mater. Struct.* **17**, 025027 (2008).

⁸S. Rafique, J. R. Cullen, M. Wuttig, and J. Cui, *J. Appl. Phys.* **95**, 6939 (2004).

⁹P. G. Evans and M. J. Dapino, *J. Appl. Phys.* **105**, 113901 (2009).